Near-Field Beam Training with Analog Extremely Large True-Time-Delay Arrays

(Invited Paper)

Ibrahim Pehlivan*, Mehmet C. Ilter†, Mikko Valkama†, and Danijela Cabric*
* Electrical and Computer Engineering Department, University of California, Los Angeles
† Department of Electrical Engineering, Tampere Wireless Research Center, Tampere University, Finland
Email: {ipehlivan, danijela}@ucla.edu, {mehmet.ilter, mikko.valkama}@tuni.fi

2024 58th Asilomar Conference on Signals, Systems, and Computers | 979-8-3503-5405-8/24/$31.00 ©2024 IEEE | DOI: 10.1109/IEEECONF60004.2024.10942936

***Abstract*—As wireless systems have started to use millimeter-wave (mmWave) frequencies to exploit the abundant bandwidth, large antenna arrays with high beamforming gain have become necessary for compensating severe path loss. However, deploying large number of antennas extends the near-field (NF) region where effective beamforming requires the knowledge of not only the user equipment (UE)'s direction, but also distance. In this paper, we present a fast NF beam training method for analog extremely large (XL) true-time-delay (TTD) arrays using only a single orthogonal frequency-division multiplexing (OFDM) pilot symbol. In the proposed virtual sub-array sparse rainbow (VSSR) algorithm, we virtually partition the antenna array into smaller aperture sub-arrays so that a UE falls in the far-field region of each sub-array. By exploiting properties of the rainbow beamforming, we obtain near-orthogonal sub-array measurements such that UE directions with respect to each sub-array can be estimated with a sparse recovery algorithm. Then, these sub-array referenced UE directions are combined to estimate UE's location. Our simulation results demonstrate that the proposed method enables near-optimal beam training using only a single OFDM symbol, achieving an average of at least the 95% of the optimal array gain under various channel conditions.**

I. Introduction

To address the diverse demands of next-generation mobile networks—spanning massive communications, ubiquitous connectivity, and integrated sensing and communication (ISAC)—mmWave frequencies and beyond are anticipated to be explored to leverage their abundant bandwidth. As these desired frequencies exhibit prohibitive path loss, extremely large aperture arrays (ELAAs) emerged as a compelling solution featuring massive number of antennas and high beamforming gain [1]. However, as the number of antennas increases, conventional assumptions on channel propagation characteristics may not hold [2].

In conventional multi-antenna systems, UE is assumed to be in far-field region with planar electromagnetic propagation characteristics. Therefore, the knowledge of the UE's direction is sufficient to properly form the high gain beam towards the UE. The boundary separating the far-field and NF regions is determined by Rayleigh distance where any UEs beyond this distance are assumed to be in the far-field region. As the Rayleigh distance is proportional to the square of the array aperture [2], the NF region expands with the growing number of antennas. So, the electromagnetic waves have to be accurately modeled as spherical waves. For example, for a uniform linear array (ULA) with 255 antennas operating at 100 GHz, the Rayleigh distance is ~ 96 meters on the boresight. Due to spherical propagation characteristics, the estimation of UE's both direction and distance is required for efficient beam alignment [3], [4]. Consequently, beam training for NF UEs may involve substantial pilot and computational overhead.

Recently, several low overhead NF beam training algorithms are proposed. In [5], authors propose a polar codebook-based compressive channel estimation algorithm using multiple OFDM pilot symbols. In [6], a two-stage hierarchical beam training method is proposed where the coarse UE direction is first estimated with conventional far-field hierarchical beam training followed by distance and direction refinement over multiple OFDM pilot symbols. Whereas, [7] estimates the direction and distance of the UE with a neural network from the output of the far-field DFT codebook. Although these methods can reduce the beam training overhead, they employ arrays with only frequency-independent phase shifters and can only create a single beam per OFDM symbol, requiring multiple OFDM pilot symbols for beam training.

TTD arrays enable low-cost frequency-dependent beamforming capabilities and can simultenously probe multiple directions with a single OFDM symbol. In [8], a far-field TTD based rainbow beamforming was proposed to perform beam training using a single OFDM pilot. This approach has been adapted to NF channels to probe multiple directions with different frequency measurements over a given path [9] or a region [10], thereby reducing the required number of pilots. Recently, sub-array based TTD architecture has been proposed [11] such that only a partition of the entire array is active per one OFDM pilot measurement. Thus, a UE that is in NF for entire array falls into the far-field region of each sub-array. Hence, beam training problem reduces to utilizing far-field rainbow beams [8] over different sub-arrays with multiple OFDM pilot symbols.

In this work, we propose a novel NF beam training algorithm using a TTD array that requires only a single OFDM pilot symbol. In the proposed method, we virtually partition the TTD array into smaller sub-arrays that effectively operate in far-field [11] while utilizing all sub-arrays simultaneously.

This material is based upon work supported by the National Science Foundation under Grant No. #2224322, and by the Research Council of Finland under the Grants #357730 and #359095.

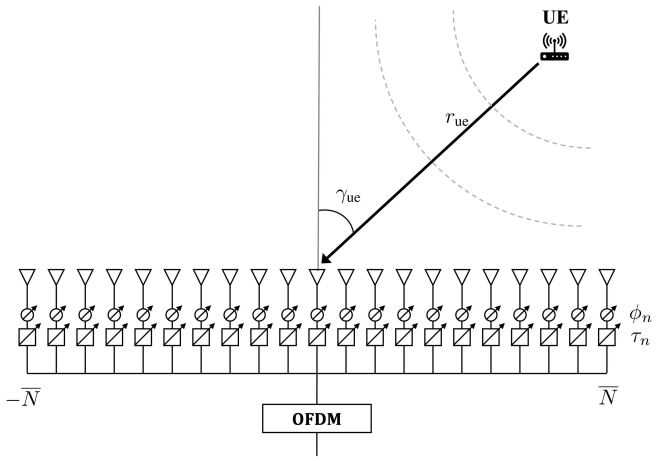

Fig. 1. Illustration of a $2\overline{N}+1$ antenna-equipped base station (BS) with a TTD array and a single antenna UE.

We then show that by utilizing simple and uniform time delay and phase values as in Rainbow beamforming [8], the received signals from different sub-arrays become near-orthogonal. As a result, UE direction referenced to each sub-array can be recovered with only a single OFDM pilot symbol. Then, by utilizing the known array structure and per sub-array UE directions, the UE's location can be angulated to enable effective beam alignment [11].

II. ELAA System Model

We consider an uplink OFDM system with a BS comprising ELAA and a single antenna UE. The system utilizes OFDM waveform operating at center frequency f_c with the total bandwidth W and $M = 2\overline{M}+1$ subcarriers. The BS centered at the origin is equipped with analog uniform linear TTD array with $N = 2\overline{N}+1$ antennas and single RF chain where each antenna $n \in [-\overline{N}, \overline{N}]$ is connected to a phase shifter, ϕ_n, and time delay element τ_n as illustrated in Fig. 1.

The UE's location is defined as $(r_{\text{ue}}, \gamma_{\text{ue}})$ where r_{ue} is the radial distance between the UE and the center of the antenna array and $\gamma_{\text{ue}} = \sin(\alpha_{\text{ue}})$ is the corresponding direction for the UE angle α_{ue}. For LOS scenario and ignoring large-scale fading, the NF channel corresponding to m-th subcarrier $\boldsymbol{h}_{m,r_{\text{ue}},\gamma_{\text{ue}}} \in \mathbb{C}^{N\times 1}$ is defined as [9]

$$[\boldsymbol{h}_{m,r_{\text{ue}},\gamma_{\text{ue}}}]_n = e^{-jk_m r_{\text{ue}}} e^{-jk_m(-nd\gamma_{\text{ue}} + n^2 d^2 \frac{1-\gamma_{\text{ue}}^2}{2r_{\text{ue}}})} \tag{1}$$

where $k_m = \frac{2\pi f_m}{c}$ is the wave number, f_m denotes the frequency of the m-th subcarrier, $f_m = f_c + W\frac{m}{M}$, and $d = \lambda_c/2$ where λ_c is the wavelength at f_c. If the UE is farther than the Rayleigh distance i.e. $r_{\text{ue}} > \frac{(N-1)^2\lambda_c}{2}$, UE's channel can be approximated as a far-field channel [2] $\boldsymbol{h}_{m,r_{\text{ue}},\gamma_{\text{ue}}} \approx \boldsymbol{h}_{m,\gamma_{\text{ue}}} \in \mathbb{C}^{N\times 1}$ where

$$[\boldsymbol{h}_{m,\gamma_{\text{ue}}}]_n = e^{-jk_m r_{\text{ue}}} e^{jk_m nd\gamma_{\text{ue}}} \tag{2}$$

where $e^{-jk_m r_{\text{ue}}}$ term is generally ignored [9]. The TTD beamforming vector for the m-th subcarrier is formulated as [11]

$$[\boldsymbol{v}_m]_n = \frac{1}{\sqrt{N}} e^{-j(2\pi f_m \tau_n - \phi_n)} \tag{3}$$

Unlike analog arrays using only frequency-independent phase shifters, the TTD array delay units enable frequency-dependent beamforming. Using conventional OFDM processing, the received signal after the combining $\boldsymbol{y}_{r_{\text{ue}},\gamma_{\text{ue}}} \in \mathbb{C}^{M\times 1}$ is given by

$$\begin{aligned}[\boldsymbol{y}_{r_{\text{ue}},\gamma_{\text{ue}}}]_m &= \boldsymbol{v}_m^H(\boldsymbol{h}_{m,r_{\text{ue}},\gamma_{\text{ue}}} + \boldsymbol{n}_m) \\ &= \sum_{n=-\overline{N}}^{\overline{N}} [\boldsymbol{v}_m]_n^*([\boldsymbol{h}_{m,r_{\text{ue}},\gamma_{\text{ue}}}]_n s_m + [\boldsymbol{n}_m]_n)\end{aligned} \tag{4}$$

where $\boldsymbol{n}_m \sim \mathcal{CN}(0, \sigma^2 \boldsymbol{I}_N) \in \mathbb{C}^{N\times 1}$ is a complex zero-mean Gaussian noise with variance σ^2 mutually independent for each m and s_m is the m-th subcarrier pilot symbol.

The objective of the beam training algorithm is to design a TTD beamforming vector $\boldsymbol{v}_m$ that is aligned with the channel vector $\boldsymbol{h}_{m,r_{\text{ue}},\gamma_{\text{ue}}}$ to maximize the received power $|\boldsymbol{v}_m^H \boldsymbol{h}_{m,r_{\text{ue}},\gamma_{\text{ue}}}|^2 |s_m|^2$ for all m. If the UE's location $(r_{\text{ue}}, \gamma_{\text{ue}})$ is known at the BS, alignment and maximum power can be achieved by configuring time delays as $\tau_n = \frac{1}{c}(-nd\gamma_{\text{ue}} + n^2 d^2 \frac{1-\gamma_{\text{ue}}^2}{2r_{\text{ue}}})$ [9] which results in:

$$\begin{aligned}|\boldsymbol{v}_m^H \boldsymbol{h}_{m,r_{\text{ue}},\gamma_{\text{ue}}}|^2 |s_m|^2 &= \frac{1}{N} |\boldsymbol{h}_{m,r_{\text{ue}},\gamma_{\text{ue}}}^H \boldsymbol{h}_{m,r_{\text{ue}},\gamma_{\text{ue}}}|^2 |s_m|^2 \\ &= N|s_m|^2\end{aligned} \tag{5}$$

In order to maximize the beamforming gain towards the UE, beam training algorithm needs to estimate the UE's location $(r_{\text{ue}}, \gamma_{\text{ue}})$ from the received signal $\boldsymbol{y}_{r_{\text{ue}},\gamma_{\text{ue}}}$.

III. Beam training with TTD Arrays

Beam training in NF channels can be achieved by aligning TTD beamforming vector towards different locations over different OFDM symbols, and probing all possible UE locations for maximum alignment. Similarly, all possible directions can be probed over different OFDM symbols for far-field channels. However, these approaches introduce considerable training overhead and do not exploit the frequency-dependent beamforming capabilities of the TTD arrays.

A. Far-field TTD Beam training

For far-field channels, it is shown that TTD arrays can probe multiple directions over different subcarriers with a single OFDM symbol, reducing the beam training overhead significantly [8]. After configuring TTD beamforming vector, as given in (3), with the following parameters

$$\tau_n = \frac{n}{W},\ \phi_n = \frac{2\pi f_c n}{W}. \tag{6}$$

the received signal $\boldsymbol{y}_{r_{\text{ue}},\gamma_{\text{ue}}}$ can be obtained as [8]

$$[\boldsymbol{y}_{r_{\text{ue}},\gamma_{\text{ue}}}]_m = \frac{e^{-jk_m r_{\text{ue}}}}{\sqrt{N}} \frac{\sin(\frac{\pi}{2} N z_{\gamma_{\text{ue}},m})}{\sin(\frac{\pi}{2} z_{\gamma_{\text{ue}},m})} \tag{7}$$

where $z_{\gamma_{\text{ue}},m} = \gamma_{\text{ue}} + m(\gamma_{\text{ue}}\frac{W}{Mf_c} + \frac{2}{M})$. It can be shown that the maximum value of $\boldsymbol{y}_{r_{\text{ue}},\gamma_{\text{ue}}}$ is attined when $\gamma_{\text{ue}} =$

$-2mf_c/(Mf_m) + 2z,\ z \in \mathbb{Z}$. Thus, the direction of the UE can be estimated as

$$\hat{m} = \arg\max |\boldsymbol{y}_{r_{\text{ue}},\gamma_{\text{ue}}}|$$
$$\hat{\gamma}_{\text{ue}} = \mod\left(1 - 2\frac{\hat{m}f_c}{Mf_m}, 2\right) - 1 \tag{8}$$

with only a single OFDM symbol. However, this approach cannot be directly applied to NF channels as TTD array configuration in (6) does not result in the received signal in (13), making straightforward subcarrier to direction mapping in (8) inapplicable.

B. Near-field sub-array TTD Beam training

Recently, sub-array based beam training method is proposed to utilize far-field rainbow TTD configuration for the NF channels [11]. As Rayleigh distance is a function of number of antennas and array aperture, the entire array can be partitioned into $S = 2\overline{S} + 1$ sub-arrays with $N_S = \frac{N}{S}$ antennas as shown in Fig. 2 such that UE falls into far-field region of every sub-array. Then by utilizing only one sub-array per OFDM symbol, each sub-array's direction γ_k can be estimated by the far-field TTD configuration described in section III-A, over multiple OFDM symbols.

Upon obtaining direction γ_k of each sub-array and utilizing known sub-array center locations in Cartesian coordinates:

$$\boldsymbol{p} = \begin{bmatrix} -\overline{S}N_S & 0 \\ \vdots & \\ \overline{S}N_S & 0 \end{bmatrix} = \begin{bmatrix} \boldsymbol{p}_x & \boldsymbol{p}_y \end{bmatrix} \in \mathbb{C}^{S\times 2} \tag{9}$$

UE's location in Cartesian coordinates $(x_{\text{ue}}, y_{\text{ue}})$ can be related to sub-array center locations as:

$$\boldsymbol{p}_x = \underbrace{\begin{bmatrix} 1 & -\tan\arcsin\gamma_{-\overline{S}} \\ & \vdots \\ 1 & -\tan\arcsin\gamma_{\overline{S}} \end{bmatrix}}_{\boldsymbol{R}} \begin{bmatrix} x_{\text{ue}} \\ y_{\text{ue}} \end{bmatrix} \tag{10}$$

and the UE's location can be estimated by following equations [11] where this procedure is termed as angulation:

$$\begin{bmatrix} x_{\text{ue}} \\ y_{\text{ue}} \end{bmatrix} = \boldsymbol{R}^{\dagger}\boldsymbol{p}_x,\ \gamma_{\text{ue}} = \sin\arctan\frac{x_{\text{ue}}}{y_{\text{ue}}},\ r_{\text{ue}} = \sqrt{x_{\text{ue}}^2 + y_{\text{ue}}^2} \tag{11}$$

where $\boldsymbol{R}^{\dagger}$ is the pseudo-inverse of $\boldsymbol{R}$ and $\boldsymbol{R}^{\dagger} = (\boldsymbol{R}^H\boldsymbol{R})^{-1}\boldsymbol{R}^H$ if $\text{rank}(\boldsymbol{R}) = 2$.

Using this sequential sub-array activation and collecting measurements using rainbow beams from each sub-array, the beam training can be achieved with S OFDM symbols. In the next section, we show that there is no need to separate measurements from each sub-array and utilize multiple OFDM symbols. In fact, by simply utilizing rainbow beam TTD configuration given in (6) direction of each sub-array can be recovered with only a single OFDM symbol.

IV. Virtual Sub-array Sparse Rainbow (VSSR) Algorithm

In this section, we show that the direction of each sub-array can be recovered with a single OFDM symbol by formulating a sparse recovery problem. As utilizing entire array is equivalent to using all sub-arrays concurrently, we first decompose the received signal from the entire array as a sum of received signals of each sub-array. By exploiting mutual near-orthogonality of sub-array signals for $S = 3$, we recover the direction of each sub-array by Orthogonal Matching Pursuit (OMP) algorithm [12]. Then, angulation method in (11) is utilized to estimate the UE's location.

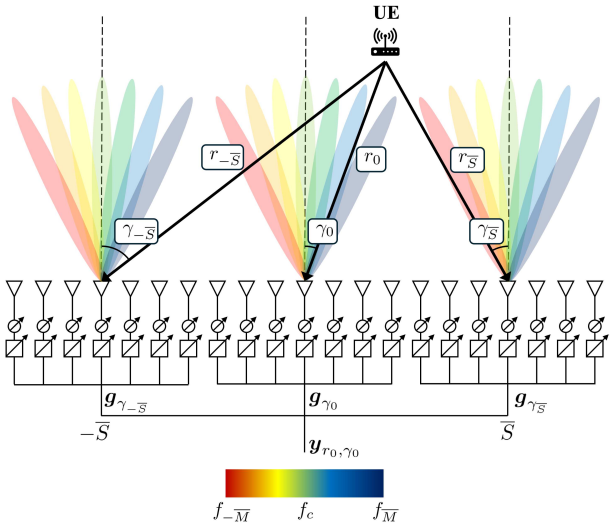

Fig. 2. Virtual partitioning of the TTD array for $S = 3$ and the VSSR algorithm rainbow beams.

A. Virtual Sub-array Signals

By exploiting the linear operations of signal combining, and inspired by the approach in Section III-B, we can mathematically partition the array into $S = 2\overline{S} + 1$ uniform sub-arrays with $N_S = 2\overline{N}_S + 1$ antennas. We refer to this operation as virtual partitioning. Then, the received signal for entire array can be written as:

$$\begin{aligned}[\boldsymbol{y}_{r_{\text{ue}},\gamma_{\text{ue}}}]_m &= \sum_{n=-\overline{N}}^{\overline{N}} [\boldsymbol{v}_m]_n^* [\boldsymbol{h}_{m,r_{\text{ue}},\gamma_{\text{ue}}}]_n \\ &= \sum_{s=-\overline{S}}^{\overline{S}} \underbrace{\sum_{n'=-\overline{N}_S}^{\overline{N}_S} [\boldsymbol{v}_m]_{n'-sN_S}^* [\boldsymbol{h}_{m,r_s,\gamma_s}]_{n'}}_{\text{Signal of sub-array } s}\end{aligned} \tag{12}$$

where $\boldsymbol{h}_{m,r_s,\gamma_s}$ is the NF channel between the UE and sub-array $s \in [-\overline{S}, \overline{S}]$, (r_s, γ_s) is the distance and direction of the UE with respect to sub-array center as illustrated in Fig. 2.

Assuming $S = 3$ and the UEs in far-field region for all virtual-sub-arrays, i.e. $\min_s(r_s) \geq \frac{(N_S-1)\lambda_c}{2}$, the received signal can further be simplified as

$$[\boldsymbol{y}_{r_{\text{ue}},\gamma_{\text{ue}}}]_m = \sum_{s=-\overline{S}}^{\overline{S}} \sum_{n'=-\overline{N}_S}^{\overline{N}_S} [\boldsymbol{v}_m^*]_{n'-sN_S} \underbrace{e^{-j(k_m r_s - k_m n d\gamma_s)}}_{[\boldsymbol{h}_{m,\gamma_s}]_{n'}} \tag{13}$$

where $\boldsymbol{h}_{m,\gamma_s}$ is the far-field channel between the UE and the s-th sub-array. From known array geometry and trigonometric identities, we can see that $r_s = \sqrt{r_{s-1}^2 + N_S^2 d^2 - 2\gamma_s r_{s-1} N_S d}$. From far field

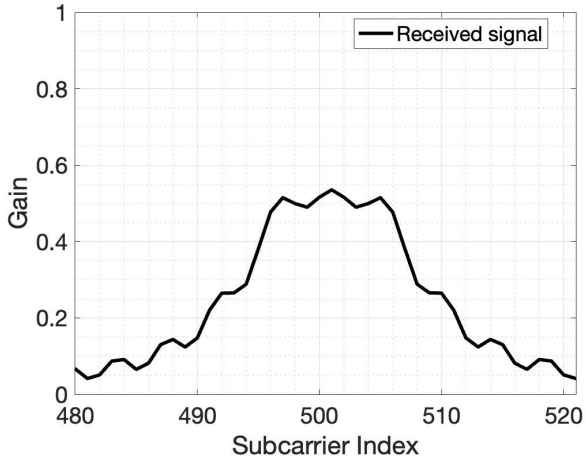

(a) Received signal gain $|\boldsymbol{y}_{r_{\text{ue}},\gamma_{\text{ue}}}|$

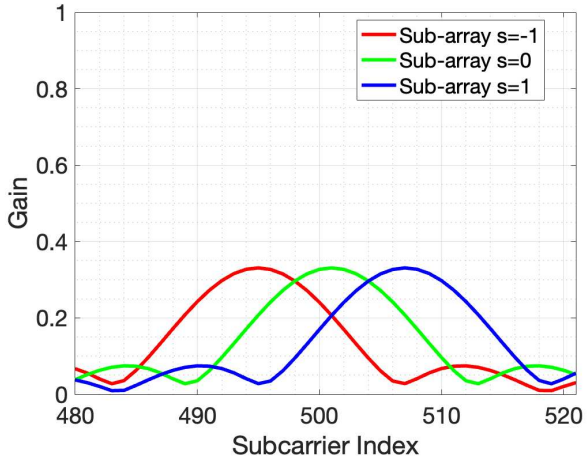

(b) Intermediate signal gain $|\boldsymbol{g}_{\gamma_s}|$, $\forall s$

Fig. 3. Gain of the received signal, in (a), and intermediate signals, in (b), for parameters $N = 255$, $S = 3$, $M = A = 1001$ and the UE is located at 10.57 meters on boresight of the ELAA.

assumption, $d(N_S - 1) \approx dN_S$ is small compared to r_s, $\forall s$ [9]; thus $r_s \approx r_{s-1} + dN_S\gamma_s$. Then, the received signal for $S = 3$ is given as:

$$[\boldsymbol{y}_{r_{\text{ue}},\gamma_{\text{ue}}}]_m = e^{-jk_m r_{\text{ue}}} \sum_{s=-\overline{S}}^{\overline{S}} \underbrace{\sum_{n'=-\overline{N}_S}^{\overline{N}_S} [\boldsymbol{v}_m]^*_{n'-sN_S} e^{jk_m(n'-sN_S)d\gamma_s}}_{[\boldsymbol{g}^s_{\gamma_s}]_m} \tag{14}$$

where $\boldsymbol{g}^s_{\gamma_s} \in \mathbb{C}^{M\times 1}$ is the intermediate signal, i.e. the received signal of the sub-array s, depending only on γ_s.

Utilizing TTD array configuration in (6), intermediate signal $\boldsymbol{g}^s_{\gamma_s}$ can be calculated as follows:

$$[\boldsymbol{g}^s_{\gamma_s}]_m = \frac{1}{\sqrt{N_S}} \sum_{n'=-\overline{N}_S}^{\overline{N}_S} e^{j\pi(n'-sN_S)(\gamma_s + \frac{2m}{M} + \frac{mW}{Mf_c}\gamma_s)} \tag{15a}$$

$$= \frac{1}{\sqrt{N_S}} \frac{\sin(\frac{\pi}{2}N_S z_{s,m})}{\sin(\frac{\pi}{2}z_{s,m})} e^{-j\pi s N_S z_{s,m}} \tag{15b}$$

where

$$z_{s,m} = \gamma_s + m(\gamma_s \frac{W}{Mf_c} + \frac{2}{M})$$

Then, the received signal $\boldsymbol{y}_{r_{\text{ue}},\gamma_{\text{ue}}}$ can be written as

$$\boldsymbol{y}_{r_{\text{ue}},\gamma_{\text{ue}}} = e^{-jk_m r_{\text{ue}}} \sum_{s=-\overline{S}}^{\overline{S}} \boldsymbol{g}^s_{\gamma_s} \tag{16}$$

Observe that the intermediate signal given in (15b) is similar to the received signal given in (13) which is the received signal of the the sub-array s of the method described in Section III-B. The only difference is the sub-array-dependent phase shift introduced by the distance between sub-array centers. Therefore, if we can recover the intermediate signal of each sub-array from the received signal $\boldsymbol{y}_{r_{\text{ue}},\gamma_{\text{ue}}}$, we can estimate the direction γ_s of each sub-array. An example of received signal and intermediate signals for parameters $N = 255$, $S = 3$, $M = A = 1001$ and a UE at 10.57 meters in the boresight is given in Fig. 3. Our goal is to recover intermediate signals illustrated in Fig. 3b from the received signal shown in Fig.3a.

Next we formulate a sparse recovery problem to recover intermediate signals and corresponding directions. To support the approach of compressive estimation, we show that the measurements from different sub-arrays are nearly-orthogonal.

B. Sparse Recovery Problem Formulation

The intermediate signal for sub-array s, $\boldsymbol{g}^s_{\gamma_i}$, is uniquely parametrized by sub-array's direction γ_s. To estimate this direction, we define a dictionary of possible directions as follows:

$$\boldsymbol{G}_s = [\boldsymbol{g}^s_{\overline{\gamma}_1}, \boldsymbol{g}^s_{\overline{\gamma}_2}, \ldots, \boldsymbol{g}^s_{\overline{\gamma}_A}] \in \mathbb{C}^{M\times A} \tag{17}$$

where for fair comparison with S-NFBT algorithm UE directions are defined as $\overline{\gamma}_a = 2\frac{af_c}{Af_m}$, $a \in [-\overline{A}, \overline{A}]$ and $A = 2\overline{A} + 1 = M$ is the number of grid directions. We estimate each sub-array's direction based on this grid. The received sub-array signal $\boldsymbol{g}^s_{\gamma_i}$ for directions on this grid can be written as:

$$\boldsymbol{g}^s_{\gamma_i} = \boldsymbol{G}_s \begin{bmatrix} 0 \\ 1 \\ \vdots \\ 0 \end{bmatrix} = \boldsymbol{G}_s \boldsymbol{x}_s \in \mathbb{C}^{M\times 1} \tag{18}$$

where $\boldsymbol{x}_s \in \mathbb{C}^{A\times 1}$ is the sparse selection vector with $\|\boldsymbol{x}_s\|_0 = 1$, $\forall s$. Therefore, we can directly obtain sub-array's direction γ_s, if we know (or have estimate of) the sparse selection vector $\boldsymbol{x}_s$ as follows

$$\begin{aligned} \hat{a} &= \arg\max |\boldsymbol{x}_s| \\ \hat{\gamma}_s &= \text{mod}\,(1 + \overline{\gamma}_{\hat{a}}, 2) - 1 \end{aligned} \tag{19}$$

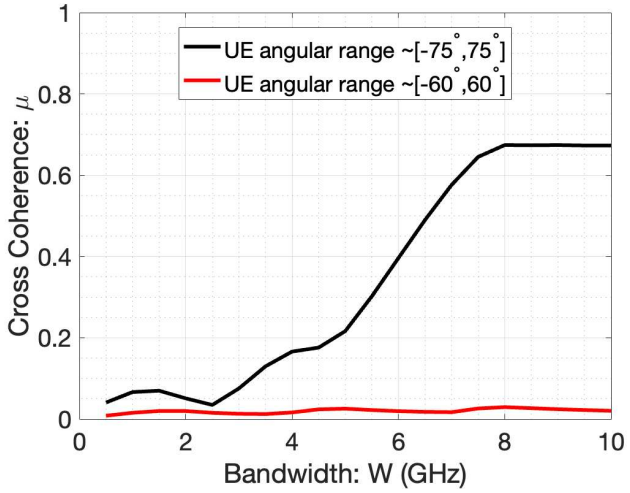

Fig. 4. The cross coherence values from (25) for two different angles of interest regions, $[-75°, 75°]$ and $[-60°, 60°]$, respectively when $W \in [1, 10]$ GHz.

Utilizing dictionary representation of intermediate signals, the received signal $\boldsymbol{y}_{r_{\text{ue}},\gamma_{\text{ue}}}$ can be written as:

$$[\boldsymbol{y}_{r_{\text{ue}},\gamma_{\text{ue}}}]_m = e^{-jk_m r_{\text{ue}}} \sum_{s=-\overline{S}}^{\overline{S}} \boldsymbol{G}_s \boldsymbol{x}_s, \quad \|\boldsymbol{x}_s\|_0 = 1, \ \forall s \tag{20}$$

Hence, we can solve the following Least Squares (LS) problem to recover sparse selection vector $\boldsymbol{x}_s$ of each sub-array [12].

$$\begin{aligned} &\min_{\boldsymbol{x}_s, \forall s} \|\boldsymbol{y}_{r_{\text{ue}},\gamma_{\text{ue}}} - \sum_{s=-\overline{S}}^{\overline{S}} \boldsymbol{G}_s \boldsymbol{x}_s\|_2 \\ &s.t. \|\boldsymbol{x_s}\|_0 = 1, \ \forall s \end{aligned} \tag{21}$$

However, obtaining the solution of (21) depends on the properties of the dictionaries $\boldsymbol{G}_s$, requiring further analysis.

1) Near-orthogonality of Sub-array Signals and Cross Coherence: We continue by showing that the intermediate signals $\boldsymbol{g}^s_{\gamma_s}$ for different sub-arrays with $S = 3$ are nearly orthogonal if the systems bandwidth W is negligible compared to f_c, making dictionaries mutually near-orthogonal.

Lemma 1. *If a system's bandwidth is negligible compared to its central frequency f_c, i.e. $W << f_c$ and number of sub-arrays is $S = 3$, the intermediate signals of different sub-arrays $k \in \{-1, 0, 1\}$ and $s \neq k \in \{-1, 0, 1\}$ are orthogonal for any direction $\gamma_i, \gamma_j \in [-1, 1]$: $\boldsymbol{g}^k_{\gamma_i} \perp \boldsymbol{g}^s_{\gamma_j}$, $\forall k, s \neq k$ & $\forall \gamma_i, \gamma_j \in [-1, 1]$*

Proof. Let us assume that fractional bandwidth of the system is very small $W << f_c$ and number of sub-arrays is $S = 3$. Then, we can approximate $z_{s,m}$ as $z_{s,m} \approx \frac{2}{M}(m + \frac{\gamma_i M}{2})$. We want to prove that the inner product between signals from different sub-arrays are orthogonal for any direction. The discrete time Fourier transform (DTFT) of the intermediate signal $[\boldsymbol{g}^s_{\gamma_s}]_m$ can be calculated as:

$$\mathcal{F}\{[\boldsymbol{g}^s_{\gamma_s}]_m\} = \Gamma_s(\Omega) = \Pi_{N_S}\left(\Omega + \frac{2\pi s N_S}{M}\right) e^{+j\Omega\frac{\gamma_s M}{2}} \tag{22}$$

along with

$$\Pi_{N_S}(\Omega) := \frac{2\pi}{\sqrt{N_S}} \sum_{m'=-\overline{N}_S}^{\overline{N}_S} \delta(\Omega - 2\pi\frac{m'}{M}) \tag{23}$$

Then, the inner product of intermediate signal of sub-array k and $s \neq k$ for respective directions γ_i, γ_j can be calculated as:

$$< \boldsymbol{g}^k_{\gamma_i}, \boldsymbol{g}^s_{\gamma_j} >= \sum_{m=-\overline{M}}^{\overline{M}} [\boldsymbol{g}^k_{\gamma_i}]^*_m [\boldsymbol{g}^s_{\gamma_j}]_m \tag{24a}$$

$$= \frac{1}{2\pi}\int_{-\pi}^{\pi} \underbrace{\Pi_{N_S}(\Omega + 2\pi\frac{kN_S}{M})^* \Pi_{N_S}(\Omega + 2\pi\frac{sN_S}{M})}_{0} e^{j\Omega\frac{(\gamma_j - \gamma_i)M}{2}} d\Omega \tag{24b}$$

$$= 0 \implies \boldsymbol{g}^k_{\gamma_i} \perp \boldsymbol{g}^s_{\gamma_j} \tag{24c}$$

where (24b) is the result of the generalized Parseval's equality [13] and (24c) is obtained from the the properties of the $\Pi_{N_S}(\Omega)$ function defined in (23). □

However, if the system has higher bandwidth W, intermediate signals are not orthogonal and inner product between intermediate signals of different sub-arrays become direction dependent. In order to quantify the coherence between intermediate signals of different sub-arrays, cross coherence metric is used [14]. This metric calculates the maximum possible coherence μ between sub-arrays out of all possible direction values in desired region, formulated as

$$\mu = \max_{\gamma_i, \gamma_j, k \neq s} |(\boldsymbol{g}^s_{\gamma_i})^H \boldsymbol{g}^k_{\gamma_j}| \tag{25}$$

Fig. 4 shows the cross coherence with respect to bandwidth for a system with $f_c = 100$ GHz, $N = 255$, $M = 1001$ and number of sub-arrays $S = 3$ for uniformly sampled directions. It can be seen that near-orthogonality is preserved across different bandwidths if UE's angular range is limited to $[-60°, 60°]$, meanwhile the orthogonality disappears for $[-75°, 75°]$ as W increases. This constraint to use directions between $[-60°, 60°]$ is common in communications systems [15] and intermediate signals can be realistically assumed to be nearly-orthogonal.

C. UE Location Estimation and Proposed Algorithm

As intermediate signals are nearly orthogonal for the region of UE directions of interest, we can utilize simplified orthogonal matching pursuit (OMP) algorithm [12] by exploiting the observed structure and solve the problem (21). Then, direction of each sub-array γ_s can be obtained from the estimated sparse selection vectors with the equation (19). Upon determining sub-array directions, UE's location can be estimated by angulation as described in (11). The proposed method is summarized in Algorithm 1 where steps [11-13] are added to address the angulation failure resulting from off-grid directions and noise. In such cases, we assume that the UE is in far-field, and direct a beam based on detected direction of center sub-array and maximum allowed UE distance, r_{max}.

Algorithm 1: VSSR algorithm

Input: Received signal, $\boldsymbol{y}_{r_{\text{ue}},\gamma_{\text{ue}}} \in \mathbb{C}^{M\times 1}$ obtained by TTD array with configuration (6),maximum UE location, $r_{\max}$

Output: UE's location, $(r_{\text{ue}}, \gamma_{\text{ue}})$

Set $\Lambda = \emptyset$, $\boldsymbol{y} = \frac{\boldsymbol{y}_{r_{\text{ue}},\gamma_{\text{ue}}}}{\|\boldsymbol{y}_{r_{\text{ue}},\gamma_{\text{ue}}}\|}$

for $s = -1 : 1$ **do**

  Create dictionary $\boldsymbol{G}_s$ as defined in (17) and normalize columns

  Obtain sparse selection vector $\hat{\boldsymbol{x}_s} = \boldsymbol{G}_s^H \boldsymbol{y}$

  Obtain direction $\hat{\gamma}_s$ from $\hat{\boldsymbol{x}_s}$ with (19)

  $\Lambda \leftarrow \Lambda \cup \{\boldsymbol{g}^s_{\hat{\gamma}_s}\}$

  $\boldsymbol{y} \leftarrow \boldsymbol{P}_{\Lambda^\perp}\boldsymbol{y}$

  $\boldsymbol{y} \leftarrow \frac{\boldsymbol{y}}{\|\boldsymbol{y}\|}$

end

Obtain UE's location from (11)

if $r_{ue} < 1e-16$ **then**

  $(r_{\text{ue}}, \gamma_{\text{ue}}) \leftarrow (r_{\max}, \hat{\gamma}_0)$

end

TABLE I
ELAA Simulation Parameters

PARAMETER	VALUE
Center frequency f_c	100 GHz
Bandwidth W	3 GHz
Number of subcarriers M	1001
Number of ULA antenna N	255
Number of sub-arrays S	3
Rayleigh distance (Boresight)	96.7 meters
Rayleigh distance of each sub-array (Boresight)	10.57 meters
UE direction grid numbers (A)	1001
UE Distances	$4 : 0.5 : 30$ meters
UE directions	$-60° : 0.5° : 60°$
SNR Values	$-10 : 10 : 30$ dB

V. Numerical Results

In this section, we demonstrate the performance of the proposed VSSR algorithm with extensive simulations where used parameters are listed in the Table I. We calculate the normalized array gain $G(r_{\text{ue}}, \gamma_{\text{ue}})$ as a performance metric defined as follows:

$$\begin{aligned} G(r_{\text{ue}}, \gamma_{\text{ue}}) &= \frac{1}{M\sqrt{N}} \sum_{m=-\overline{M}}^{\overline{M}} |\boldsymbol{v}_m \boldsymbol{h}_{m,r_{\text{ue}},\gamma_{\text{ue}}}| \\ &= \frac{1}{M\sqrt{N}} \sum_{m=-\overline{M}}^{\overline{M}} |\boldsymbol{h}_{m,\hat{r}_{\text{ue}},\hat{\gamma}_{\text{ue}}} \boldsymbol{h}_{m,r_{\text{ue}},\gamma_{\text{ue}}}| \end{aligned} \tag{26}$$

where $(r_{\text{ue}}, \gamma_{\text{ue}})$ is the actual and $(\hat{r}_{\text{ue}}, \hat{\gamma}_{\text{ue}})$ is the estimated UE location and $\boldsymbol{v}_m$ is configured as in (5) and pre-beamforming noise variance is $\sigma^2 = \frac{1}{\text{SNR}}$.

The following benchmark beam training schemes are utilized in the subsequent performance comparison:

1) S-NFBT algorithm [11]: This is the sequential sub-array rainbow algorithm described in Section III-B. The required number of OFDM symbols for this algorithm is $S = 3$.

2) Dictionary-based S-NFBT (DS-NFBT) algorithm: To provide a fair comparison, we extend the S-NFBT algorithm [11] with a dictionary based approach and estimate each sub-array's direction with(18) and (19) rather than (8). Note that the required number of the OFDM symbols is the same as in S-NFBT benchmark.

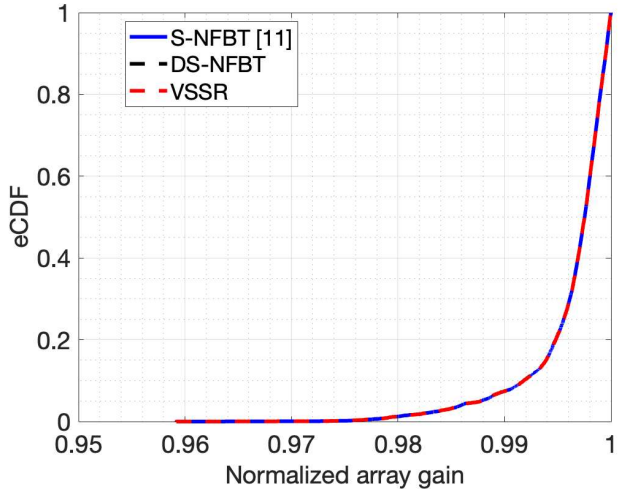

Fig. 5. The empirical CDF comparison of S-NFBT [11], dictionary-based S-NFBT (DS-NFBT) and VSSR algorithms in terms of the normalized array gain when the noise-free cases are considered.

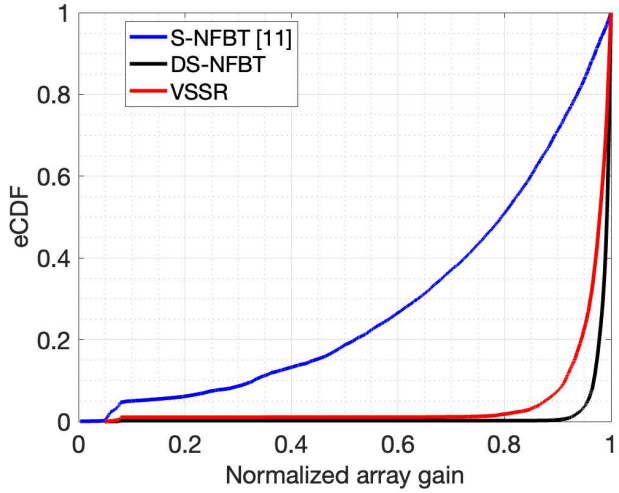

Fig. 6. The empirical CDF comparison of the normalized array gain between S-NFBT [11], dictionary-based S-NFBT (DS-NFBT) and VSSR algorithms when pre-beamforming SNR is set to -10 dB.

Fig. 5 shows the empirical CDF of the normalized array gains with respect to different UE locations for the noise-free scenario. Results indicate that the VSSR algorithm performs identical to the SDR algorithm and to benchmark S-NFBT algorithm, verifying that the intermediate signal of each sub-array can be recovered with only a single OFDM symbol.

Similarly, Fig. 6 shows the empirical CDF of the normalized array gains of different UE locations when pre-beamforming SNR is -10 dB. Even under this channel condition, VSSR and DS-NFBT perform near-optimal, providing at least 93% of the optimal array gain for 85% and 98% of the locations, respectively. The presented results solidify that VSSR can achieve reliable beam training with a single OFDM symbol even under low SNR range. Both dictionary based algorithms outperform S-NFBT as the projection over dictionary vectors improves SNR.

TABLE II
Percentage of angulation failure for different SNR and sensitivity conditions for S-NFBT [11], DS-NFBT and VSSR algorithms.

Detection of $r_{\text{ue}} < 1e-16$			
SNR (dB)	S-NFBT [11]	DS-NFBT	VSSR
-10	0.5533%	0.3336%	0.5858%
0	0.7404%	0.0244%	0.0651%
10	0.5858%	0%	0%
20	0.2034%	0%	0%
30	0.0325%	0%	0%
∞	0%	0%	0%
Detection of $r_{\text{ue}} < 1e-1$			
SNR (dB)	S-NFBT [11]	DS-NFBT	VSSR
-10	4.7270%	0.5533%	1.6435%
0	2.8720%	0.0244%	0.0814%
10	1.3750%	0%	0%
20	0.2766%	0%	0%
30	0.0325%	0%	0%
∞	0%	0%	0%

Table II demonstrates the angulation failure percentage for different SNR values and different tolerances. Due to noise and finite direction grid resolution, all algorithms can detect same or unrealistic directions for different sub-arrays, making algorithms fail to angulate and return UE location as $(0, 0)$. We treat these cases as if UE is in far-field and if $\hat{r}_{\text{ue}} < \textit{tolerance}$ we assign UE the location $(r_{\max}, \hat{\gamma}_{\text{ue}})$ where $\hat{\gamma}_0$ is the estimated direction of the center sub-array and $r_{\max}$ is the maximum possible UE distance. The presented results demonstrate that both VSSR and DS-NFBT is resilient to such errors due to additional gain from projection to dictionary vectors. Failure percentage can further be reduced by increasing the number of directiongrid points M for S-NFBT and A for VSSR and DS-NFBT, respectively.

Fig. 7 shows the average normalized array gain over different set of UE locations for different SNR ranges. Across all SNR conditions, VSSR and SDR achieve near-optimal beam training performance, providing an average of more than 95% of the optimal array gain. Furthermore, VSSR improves the averagenormalized array gain of the S-NFBT by $\sim$ 33% at SNR$= -10$ dB while requiring only a single OFDM symbol.

VI. Conclusion

In this work, we proposed a single OFDM pilot symbol NF beam training algorithm utilizing rainbow beams with analog TTD array. We showed that by utilizing far-field rainbow beam configuration in NF and virtually partitioning the array, the received signal can be expressed as a superposition of near-orthogonal signals from each sub-array. Based on this observation, we developed an algorithm to recover each sub-array's direction by formulating a sparse recovery problem, and angulate the UE's location for effective beam alignment. Our simulation results demonstrated that the proposed method achieves near-optimal beamforming gain performance even under low SNR conditions. In the future, we are planning to investigate the multi-user scenarios and the design of different virtual partitioning of the XL TTD , and utilization of machine learning (ML) for localization and tracking in NF region.

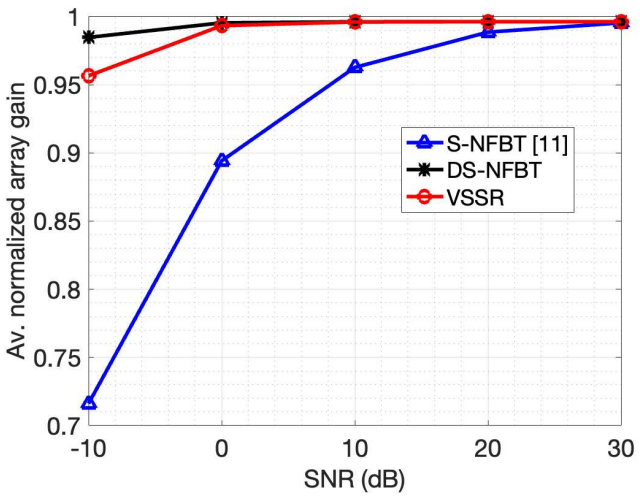

Fig. 7. Average normalized array gain after beam training with S-NFBT [11], DS-NFBT and VSSR algorithms for different SNR values.

References

[1] S. Ye, M. Xiao, M.-W. Kwan, Z. Ma, Y. Huang, G. Karagiannidis, and P. Fan, "Extremely large aperture array (ELAA) communications: Foundations, research advances and challenges," *IEEE Open J. Commun. Soc.*, vol. 5, pp. 7075–7120, 2024.

[2] Y. Liu, Z. Wang, J. Xu, C. Ouyang, X. Mu, and R. Schober, "Near-field communications: A tutorial review," *IEEE Open J. Commun. Soc.*, vol. 4, pp. 1999–2049, 2023.

[3] Z. Wu and L. Dai, "Multiple access for near-field communications: SDMA or LDMA?" *IEEE J. Select. Areas Commun.*, vol. 41, no. 6, pp. 1918–1935, 2023.

[4] S. Hu, H. Wang, and M. C. Ilter, "Design of near-field beamforming for large intelligent surfaces," *IEEE Trans. Wireless Commun.*, vol. 23, no. 1, pp. 762–774, 2024.

[5] M. Cui and L. Dai, "Channel estimation for extremely large-scale MIMO: Far-field or near-field?" *IEEE Trans. Commun.*, vol. 70, no. 4, pp. 2663–2677, 2022.

[6] C. Wu, C. You, Y. Liu, L. Chen, and S. Shi, "Two-stage hierarchical beam training for near-field communications," *IEEE Trans. Veh. Technol.*, vol. 73, no. 2, pp. 2032–2044, 2024.

[7] W. Liu, H. Ren, C. Pan, and J. Wang, "Deep learning based beam training for extremely large-scale massive MIMO in near-field domain," *IEEE Commun. Lett.*, vol. 27, no. 1, pp. 170–174, 2023.

[8] H. Yan, V. Boljanovic, and D. Cabric, "Wideband millimeter-wave beam training with true-time-delay array architecture," in *Proc. Asilomar Conf. Signals, Systems & Computers*, Pacific Grove, USA, 2019, pp. 1447–1452.

[9] M. Cui, L. Dai, Z. Wang, S. Zhou, and N. Ge, "Near-field rainbow: Wideband beam training for XL-MIMO," *IEEE Trans. Wireless Commun.*, vol. 22, no. 6, pp. 3899–3912, 2023.

[10] T. Zheng, M. Cui, Z. Wu, and L. Dai, "Near-field wideband beam training based on distance-dependent beam split," 2024. [Online]. Available: https://arxiv.org/abs/2406.07989

[11] S. Shin, J. Moon, S. Kim, and B. Shim, "Subarray-based near-field beam training for 6G terahertz communications," in *Proc. IEEE Int. Conf. Commun. (ICC)*, Denver, USA,2024, pp. 3189–3194.

[12] C. Herzet, A. Drémeau, and C. Soussen, "Relaxed recovery conditions for omp/ols by exploiting both coherence and decay," *IEEE Trans. Inf. Theory*, vol. 62, no. 1, pp. 459–470, 2016.

[13] M. Vetterli, J. Kovačević, and V. K. Goyal, *Foundations of signal processing*. Cambridge University Press, 2014.

[14] P. Sprechmann, I. Ramirez, G. Sapiro, and Y. C. Eldar, "C-hilasso: A collaborative hierarchical sparse modeling framework," *IEEE Trans. Signal Process.*, vol. 59, no. 9, pp. 4183–4198, 2011.

[15] "3GPP TS 38.213: NR; Physical layer procedures for control," 3rd Generation Partnership Project (3GPP), Tech. Rep., Sep. 2024, version 17.3.0, Release 17. [Online]. Available: https://www.3gpp.org/DynaReport/38213.htm